The Chaotic Mobile Robot

Akinori Sekiguchi and Yoshihiko Nakamura

Dept. of Mechano-Informatics, University of Tokyo
7-3-1 Hongo, Bunkyo-Ku, Tokyo 113-8656, Japan

ABSTRACT

In this paper, we develop a method to impart the chaotic nature to a mobile robot. The chaotic mobile robot implies a mobile robot with a controller that ensures chaotic motions. Chaotic motion is characterized by the topological transitivity and the sensitive dependence on initial conditions. Due to the topological transitivity, the chaotic mobile robot is guaranteed to scan the whole connected workspace. For scanning motion, the chaotic robot neither requires the map of workspace nor plans the global motion. It only requires to measure the local normal of the workspace boundary when it comes close to it. We design the controller such that the total dynamics of mobile robot is represented by the Arnold equation, which is known to show the chaotic behavior of non-compressive perfect fluid. Experimental results and their analysis illustrate the usefulness of the proposed controller.

Keywords: Chaos, Mobile Robot, Nonlinear Dynamics, Arnold Equation, Topological Transitivity

1 INTRODUCTION

Chaos characterizes one of mysterious rich behaviors of nonlinear dynamical systems. A lot of research efforts have been paid to establish the mathematical theory behind chaos. Applications of chaos are also being studied and include, for example, controlling chaos[1][2], and chaotic neural networks[3].

This paper proposes a method to impart chaotic behavior to a mobile robot. This is achieved by designing a controller which ensures chaotic motion. The topological transitivity * property of chaotic motions guarantees a complete scan of the whole connected workspace. The proposed scheme neither requires a map of workspace nor plans a path through it. It only requires the measurement of the local normal of the boundary when it comes close to it.

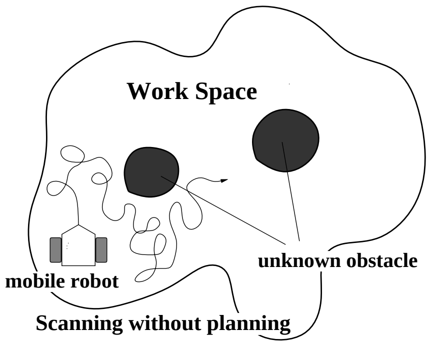

Fig. 1: Chaotic patrol

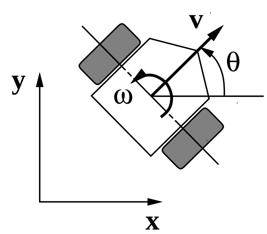

Fig. 2: Mobile robot

A mobile robot with such characteristics may find its applications as a patrol robot or a cleaning robot in a closed room, floor, or building (Fig. 1). The sensitive dependence on initial condition also yields a favourable nature as a patrol robot since the scanning trajectory becomes highly unpredictable.

2 CHAOTIC MOBILE ROBOT WITH THE ARNOLD EQUATION

2.1 Mobile Robot

As the mathematical model of mobile robots, we assume a two-wheeled mobile robot as shown in Fig. 2. Let the linear velocity of the robot v[m/s] and the angular velocity ω[rad/s] be the inputs to the system. The state equation of the mobile robot is written as follows:

$$\begin{pmatrix} \dot{x} \\ \dot{y} \\ \dot{\theta} \end{pmatrix} = \begin{pmatrix} \cos\theta & 0 \\ \sin\theta & 0 \\ 0 & 1 \end{pmatrix} \begin{pmatrix} v \\ \omega \end{pmatrix} \tag{1}$$

* Consider $\boldsymbol{C}^r (r \geq 1)$ autonomous vector fields on $\boldsymbol{R}^n$ denoted as follows.

$$\dot{x} = f(x)$$

Let the flow generated by this equation be denoted as $\phi(t, x)$ and let $\Lambda \subset \boldsymbol{R}^n$ be a invariant compact set for this flow. A closed invariant set Λ is said to be topologically transitive[5] if, for any two open sets $U, V \subset \Lambda$,

$$^{\exists}t \in \boldsymbol{R}, {^{\exists}}\phi(t, U) \cap V \neq \emptyset$$

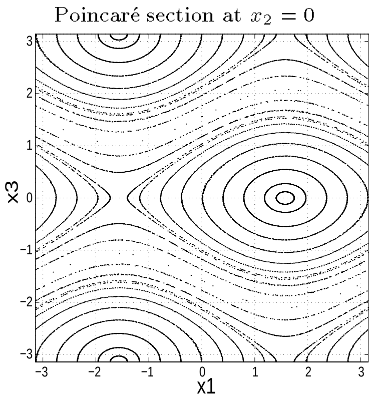

Fig. 3: Poincaré section of Arnold flow ($A = 1, B = 0.5,\ C = 0$)

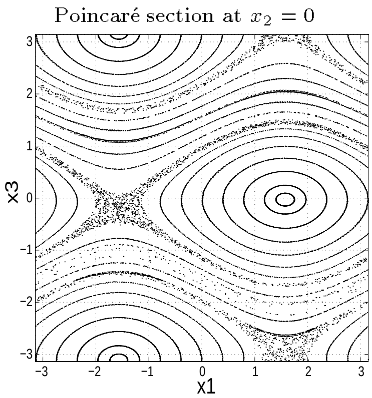

Fig. 4: Poincaré section of Arnold flow ($A = 1, B = 0.5,\ C = 0.05$)

where (x[m], y[m]) is the position of the robot, θ[rad] is the angle of the robot.

2.2 The Arnold Equation

In order to generate chaotic motions of the mobile robot, we employ the Arnold equation, which is written as follows:

$$\begin{pmatrix} \dot{x}_1 \\ \dot{x}_2 \\ \dot{x}_3 \end{pmatrix} = \begin{pmatrix} A\sin x_3 + C\cos x_2 \\ B\sin x_1 + A\cos x_3 \\ C\sin x_2 + B\cos x_1 \end{pmatrix} \tag{2}$$

where A, B and C are constants. The Arnold equation is one of steady solutions of 3-dimensional Euler equation:

$$\frac{\partial v_i}{\partial t} + \sum_{k=1}^{3} v_k \frac{\partial v_i}{\partial x_k} = -\frac{1}{\rho}\frac{\partial p}{\partial x_i} + f_i \tag{3}$$

$$\sum_{i=1}^{3} \frac{\partial v_i}{\partial x_i} = 0 \tag{4}$$

which expresses the behaviors of non-compressive perfect fluids on a 3-dimensional torus space. (x_1, x_2, x_3) and (v_1, v_2, v_3) denote the position and velocity of a particle, and p, (f_1, f_2, f_3) and ρ denote the pressure, external force, and density, respectively. It is known that the Arnold equation shows periodic motion when one of the constants, for example C, is 0 or small, and shows chaotic motion when C is large[4].

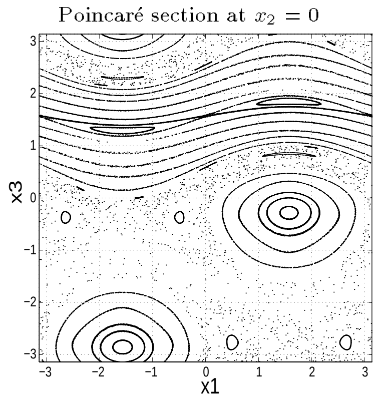

Fig. 5: Poincaré section of Arnold flow ($A = 1, B = 0.5,\ C = 0.5$)

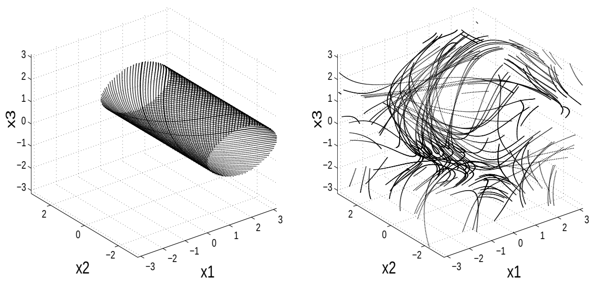

(a) $A = 1, B = 0.5, C = 0$
initial state:
$x_1 = 0, x_2 = 0, x_3 = 0$

(b) $A = 1, B = 0.5, C = 0.5$
initial state:
$x_1 = 4, x_2 = 3.5, x_3 = 0$

Fig. 6: Arnold flow

The Poincaré Section: We compose Poincaré sections[5] of the Arnold equation by numerical computation. The results are shown in Figs. 3, 4 and 5. The sections and coefficients of the Arnold equation are shown in Table 1. Figures 6(a) and (b) show trajectories of the Arnold equation in a 3-dimensional torus space, corresponding to Figs. 3 and 5 respectively.

Figure 3 represents the Poincaré section when $C = 0$. It is observed that the topological transitivity does not emerge in this case, since trajectories in the Poincaré section are closed. When $|C|$ exceeds a

Table 1: Parameters for computations

	coefficients	section
Fig.3	$A = 1, B = 0.5, C = 0$	$x_2 = 0$
Fig.4	$A = 1, B = 0.5, C = 0.05$	
Fig.5	$A = 1, B = 0.5, C = 0.5$	

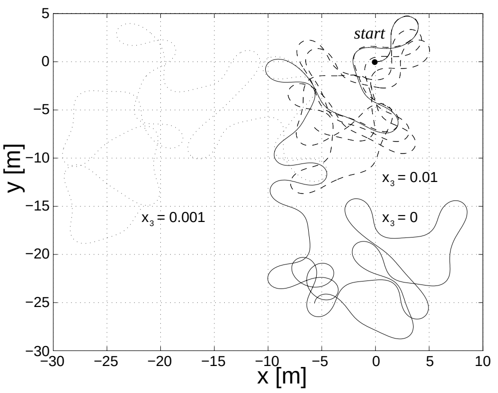

initial state	$x = 0$ [m], $y = 0$ [m]
solid line :	$x_1 = 0, x_2 = 0, x_3 = 0$
dotted line :	$x_1 = 0, x_2 = 0, x_3 = 0.001$
broken line :	$x_1 = 0, x_2 = 0, x_3 = 0.01$

Fig. 7: Trajectories of the mobile robot in x-y plane ($v = 1$, $A = 1, B = 0.5, C = 0.5$)

certain small number and gets larger, there grow regions in which closed trajectories disappear and scattered discrete points appear. The regions characterize chaos and its behavior. Since the Arnold equation is a conservative system, it is an important feature that the descrete trajectory of a point initially started in such a region remains there and is never attracted by the closed trajectories outside the region.

The Lyapunov Exponent: The Lyapunov exponent is used as a measure of the sensitive dependence on initial conditions, that is one of two characteristics of chaotic behavior[6]. There are n Lyapunov exponents in an n dimensional state space, and the system is concluded to have the sensitive dependence on initial conditions when the maximum Lyapunov exponent is positive.

We calculated the Lyapunov exponents of the Arnold equation. The parameters and the initial states are as follows:

coefficients	:	$A = 0.5, B = 0.25, C = 0.25$
initial states	:	$x_1 = 4, x_2 = 3.5, x_3 = 0$

and the Lyapunov exponents are

$$\lambda_1 = 4.3 \times 10^{-2}$$
$$\lambda_2 = 1.1 \times 10^{-4}$$
$$\lambda_3 = -4.3 \times 10^{-2}$$

Since the maximum exponent λ_1 is positive, the Arnold equation has the sensitive dependence on initial conditions.

In case of the Arnold flow, the sum of the Lyapunov exponents, $\lambda_1 + \lambda_2 + \lambda_3$, equals zero since the volume in the state space is conserved. This results in the fact that a trajectory which started from a chaotic region will not be attracted into attractors like limit cycles. The total of the computed Lyapunov exponents became slightly larger than zero, which is due to the numerical computation error.

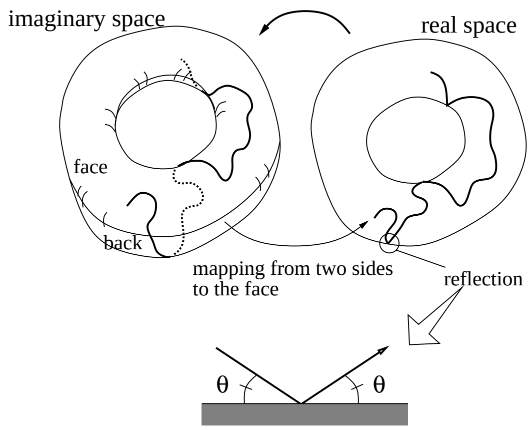

Fig. 8: Mirror mapping

2.3 Implementation of the Arnold Equation

In order to implement the Arnold equation into the controller of the mobile robot, we define and use the following state variables:

$$\begin{cases} \dot{x}_1 = D\dot{y} + C\cos x_2 \\ \dot{x}_2 = D\dot{x} + B\sin x_1 \\ x_3 = \theta \end{cases} \tag{5}$$

where B, C and D are constants. Substituting Eq. (1) in the above, we obtain a state equation on x_1, x_2 and x_3 as follows:

$$\begin{cases} \dot{x}_1 = Dv\sin\theta + C\cos x_2 \\ \dot{x}_2 = Dv\cos\theta + B\sin x_1 \\ \dot{x}_3 = \omega \end{cases} \tag{6}$$

We now design the inputs as follows:

$$\begin{cases} v = \frac{A}{D} \\ \omega = C\sin x_2 + B\cos x_1 \end{cases} \tag{7}$$

Consequently, the state equation of the mobile robot becomes

$$\begin{pmatrix} \dot{x}_1 \\ \dot{x}_2 \\ \dot{x}_3 \\ \dot{x} \\ \dot{y} \end{pmatrix} = \begin{pmatrix} A\sin x_3 + C\cos x_2 \\ B\sin x_1 + A\cos x_3 \\ C\sin x_2 + B\cos x_1 \\ v\cos x_3 \\ v\sin x_3 \end{pmatrix} \tag{8}$$

Equation (8) includes the Arnold equation. The Arnold equation behaves chaotic or not chaotic depending upon the initial states. We choose the initial states of the Arnold equation such that the trajectory should behave chaotic. As explained in section 2.2, it is guaranteed that a chaotic orbit of the Arnold equation is not attracted to a limit cycle or a quasiperiodic orbit.

The whole states evolve in a 5-dimensional space according to Eq. (8), which includes a 3-dimensional subspace of the Arnold flow. The state evolution in the two-dimensional complementary space is highly coupled with that in the three-dimensional subspace

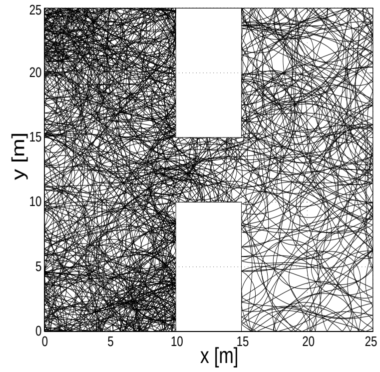

Fig. 9: Simulated trajectory of the mobile robot in x-y plane (Environment 1)

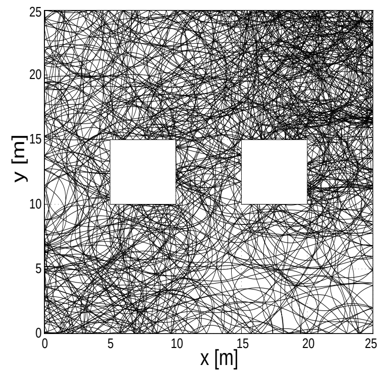

Fig. 10: Simulated trajectory of the mobile robot in x-y plane (Environment 2)

as seen in Eq. (8). The coupling is physically interpreted by the fact that the mobile robot moves with a constant velocity and being steered by the third variable of the Arnold equation. Although it is likely that the trajectory in the x-y space also behaves chaotic, it is difficult to prove. The nature of the mobile robot trajectory is to be numerically evaluated in the following section.

Figure 7 shows an example of motions of the mobile robot with the proposed controller, obtained by numerical simulation. The initial condition was chosen from a region where the Poincaré section forms no closed trajectory. It is observed that the motion of the robot is unpredictable, and sensitively dependent on initial conditions.

In Eq. (8), it is assumed that the robot moves in a smooth state space with no boundary. However, a real robot moves in spaces with boundaries like walls or surfaces of obstacles. To solve this problem, we consider the motion of the robot in an imaginary space as shown in Fig. 8. This imaginary space is obtained by smoothly connecting boundaries of two spaces that have the same shape as the real space. The mobile robot moves on the surface of this imaginary space. The trajectory of the mobile robot in real space is obtained by mapping from two sides in imaginary space to the real side. Since the robot moves as if it is reflected by the boundary, we call this method the "mirror mapping".

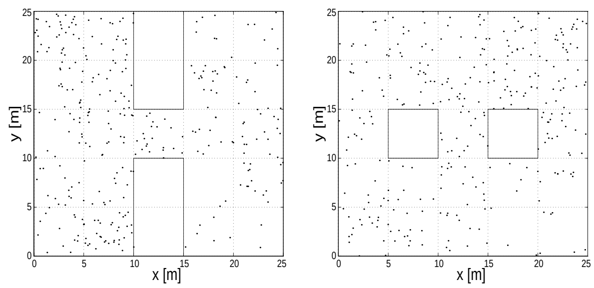

(a) Environment 1 (b) Environment 2

Fig. 11: Poincaré map of the simulation at $x_3 = \pi/4$

3 NUMERICAL ANALYSIS OF THE BEHAVIOR OF ROBOT

We investigate by numerical analysis whether the mobile robot with the proposed controller actually behaves chaotic. Examples of trajectories of the robot are obtained applying the mirror mapping, and shown in Figs. 9 and 10. The parameters and the initial states used are as follows:

coefficients	:	$v = 1$ [m/s], $A = 0.5$ [1/s]
		$B = 0.25$ [1/s], $C = 0.25$ [1/s]
initial states	:	$x_1 = 4, x_2 = 3.5, x_3 = 0$
		$x = 5$ [m], $y = 5$ [m]
period	:	8000 [s]

The trajectories generated by Eq. (8) scanned the whole workspace regardless of the shape of workspace.

Figures 11(a) and (b)show the Poincaré sections at $x_3 = \pi/4$ obtained from Figs. 9 and 10. The descrete points are distributed over the whole workspace, which indicates that the motion generated by the proposed controller shows the topological transitivity in the workspaces.

We calculated the Lyapunov exponents of the robot. Three Lyapunov exponents on the trajectory in 3-dimensional space (x, y, x_3) projected from 5-dimensional state space of Eq. (8), became as follows:

$$\lambda_1 = 1.2 \times 10^{-2}$$
$$\lambda_2 = -6.6 \times 10^{-5}$$
$$\lambda_3 = -6.9 \times 10^{-4}$$

The maximum exponent, λ_1, is positive and, therefore, the motion of robot possesses the sensitive dependence on initial conditions.

From the numerical computations, we can conclude that the motion of the robot due to the proposed controller is chaotic.

Fig. 12: Prototype mobile robot

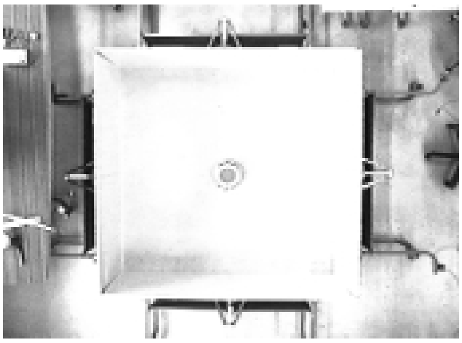

Fig. 13: Experimental environment

4 EXPERIMENT

We made experiments using a two-wheeled mobile robot shown in Fig. 12 and setting up an experimental environment (1.8m $\times$ 1.8m) shown in Fig. 13. The robot has 6 proximity sensors at the front. The mirror mapping is applied based on the information.

The chaotic mobile robot ran with the following conditions:

linear velocity	:	$v = 12$ [cm/sec]
coefficients	:	$A = 0.27$ [1/s], $B = 0.135$ [1/s]
		$C = 0.135$ [1/s]
initial states	:	$x_1 = 4, x_2 = 3.5, x_3 = 0$
period	:	2 hours

The result is shown in Fig. 14, which was obtained by tracking the robot using a camera above the experimental environment. The robot successfully scanned the whole workspace.

5 DISCUSSION: CHAOS VS. RANDOMNESS

Random walk is known as another method to scan some workspace without the map. We need to discuss the usefulness of the chaotic mobile robot as compared with random walk. We also ran the robot for 2 hours by using random walk. Random walk was implemented in such a way that the robot turns toward random direction after moving straight for every

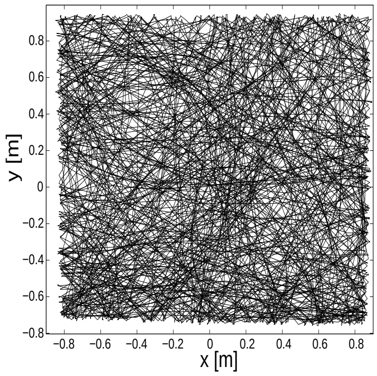

Fig. 14: Resultant trajectory of the experiment (chaotic robot)

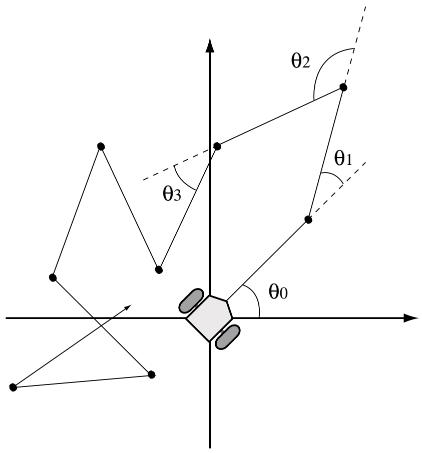

Fig. 15: Random walk

2 seconds (Fig. 15). The experimental environment and the constant velocity of the robot were the same as those of the previous experiment. The mirror mapping was also applied at boundaries.

Figure 16 shows the result. The density of resultant trajectory of random walk is lower than that of the chaotic robot, that is because the robot must spend time to stop and turn after moving for 2 seconds. It is one of advantages of the proposed controller that the robot can move continuously with the constant linear velocity.

Figures 17 and 18 are plots of the position of robot after every 1 second during every 10 minutes. It can be seen that the chaotic mobile robot in Fig. 17 could scan the workspace more efficiently. Figure 19 shows the growth of the ratio of covered area by the robot to the whole area. The chaotic mobile robot could cover 90 percent of the whole area in one third of the time taken by random walk to cover the same area.

There are many different ways to integrate random walk. Therefore, the above conclusion is not in any sense general. However, there is a possibility that the chaotic scan is stochastically superior to the scan by randomness. On the manifold integral calculus by the Monte Carlo method, Umeno[7]

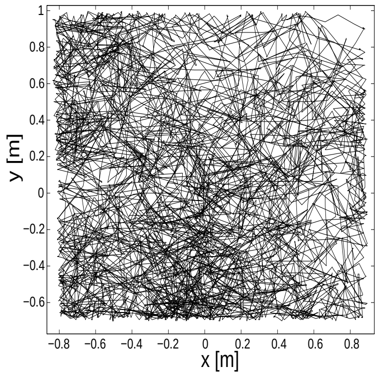

Fig. 16: Resultant trajectory of the experiment (random walk)

made a comparison between the algorithm using an exactly solvable chaos and the conventional algorithm using random numbers, and showed superiority of the chaos computing. He explained that long-term correlation and non-Gaussian nature of chaos could play important roles in this problem. Our problem of scanning the whole connected workspace is considered as a Monte Carlo computing to get the square measure of the workspace. The chaotic mobile robot has a chance being sperior to random walk, although the Arnold equation in the proposed controller is not an exactly solvable chaos. Our experiments with analysis of Figs. 17 and 18 clearly showed that the chaotic mobile robot is superior to an algorithm of random walk in efficiency of scanning the workspace.

6 CONCLUSION

In this paper, we have proposed the chaotic mobile robot, which implies a mobile robot with a controller that ensures chaotic motion. We designed the controller such that the total dynamics of mobile robot is represented by the Arnold equation. Experimental results illustrated the usefulness of the proposed controller.

This research was conducted under "Robot Brain Project" (PI: Y. Nakamura, Univ. of Tokyo) being supported by the CREST Program of the Japan Science and Technology Corporation.

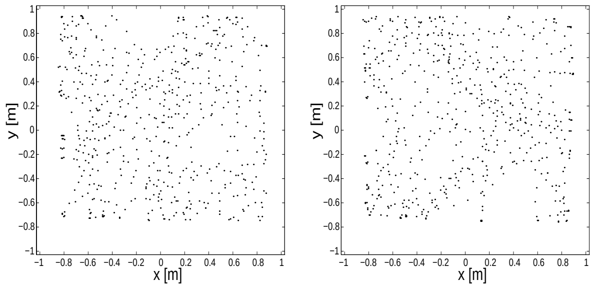

(a) $t = 0, \cdots, 10$ [min] (b) $t = 10, \cdots, 20$ [min]

Fig. 17: Plots of robot position at every 10 minutes intervals (chaotic robot)

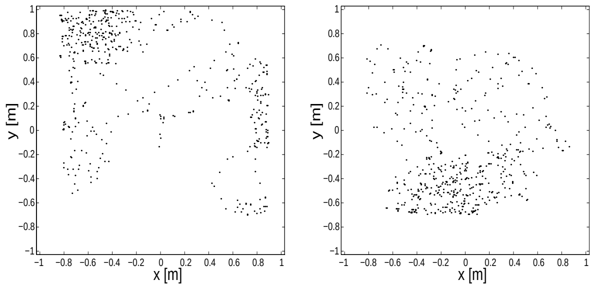

(a) $t = 0, \cdots, 10$ [min] (b) $t = 10, \cdots, 20$ [min]

Fig. 18: Plots of robot position at every 10 minutes intervals (random walk)

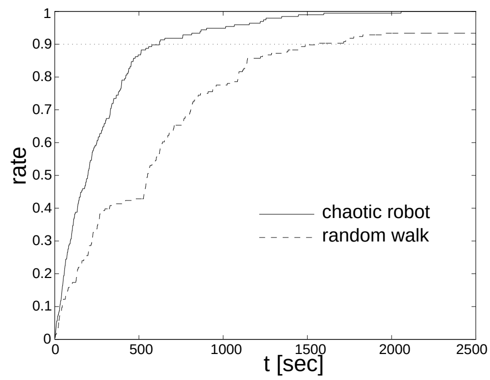

Fig. 19: Rate of covered area

References

[1] E. Ott, C. Grebogi, and J. A. Yorke: "Controlling Chaos", Physical Review Letters, Vol.64, No.11, pp.1196-1199, 1990.

[2] T. Ushio: "Chaotic synchronization and controlling chaos based on contraction mappings", Physics Letters A, Vol.198, No.1, pp.14-22, 1995.

[3] K. Aihara, T. Takabe and M. Toyoda: "Chaotic Neural Networks", Physics Letters A, Vol.144, No.6,7, pp.333-340, 1990.

[4] H. Okamoto, H. Fujii: "Nonlinear Dynamics", Iwanami Lectures of Applied Mathematics, Vol.14, Iwanami, Tokyo, 1995 (in Japanese).

[5] S. Wiggins: "Introduction to Applied Nonlinear Dynamical Systems and Chaos", Springer-Verlag, 1990.

[6] G. L. Baker and J. P. Gollub: "Chaotic Dynamics an introduction", Cambridge University Press, 1990.

[7] K. Umeno: "Chaos and Computing", Mathematical Science, No.415, pp.60-68, Jan. 1998 (in Japanese).